A SIMULATION OF EVAPORATION DISSOLUTION PROCESS FOR A LYOCELL SOLUTION IN A VERTICAL WIPED FILM EVAPORATOR (1: SIMULATION OF FLOW PROCESS FOR SOLUTION)

CHOL-JUN RI,[*] YON-CHOL KIM,[**] SUNG-WON KIM[**] and JONG-HYOK CHOE[*]

[*]*Department of Industrial Measurement No.2, Institute of Automation, Unjong District, Pyongyang, Democratic People's Republic of Korea*
[**]*Department of Computational Mathematics, Institute of Mathematics, Unjong District, Pyongyang, Democratic People's Republic of Korea*
✉ *Corresponding author*: *C. J. Ri, rcj1982@star-co.net.kp*

Received November 10, 2022

Vertical wiped film evaporators (VWFE) have found wide application in chemical, food and especially, fiber industries. In this paper, a mathematical simulation is represented for the vacuum evaporation dissolution process of Lyocell solution (reed cellulose, N-Methylmorpholine N-oxide (NMMO) solvent, water) in VWFE. The Turbulent Flow model in geometries with rotating parts and the frozen rotor approach in COMSOL Multi-physics 5.4 were used for simulation of the solution flow in VWFE. Comparing the obtained simulation results with experimental details, we show the effect of our simulation method.

Keywords: Lyocell solution, vertical wiped film evaporator, evaporation dissolution, simulation, residence time

INTRODUCTION

Evaporation is an operation used to remove liquid from a solution, suspension or emulsion by boiling off a fraction of the liquid. The steady state operation of evaporators for evaporation and dissolution is one of the most energy intensive processes in the fiber industries. So, the selection of an evaporator should be done carefully, therefore, various types of evaporators have been used in fiber, chemical and food industries.

Vertical wiped film evaporators (VWFEs) have been studied intensively all over the world, as they have the advantage of shorter evaporation dissolution time, compared to horizontal evaporators. In the Lyocell process, a VWFE is used to remove excess water from the mixture of cellulose, water and NMMO solvent.[1] For easy understanding of the operation process in the evaporator, in Figure 1, the general structure of the VWFE is shown.

Several papers have been reported in the literature for the simulation of the evaporation dissolution process in the VWFE.[2] A mathematical model and associated computer program were used to simulate the steady state operation of wiped film evaporators for the dissolution of a glycerol-water solution and the evaluation of solution dissolution according to the changes in feed rate and rotor speed.[3]

The simulation of the Lyocell process was also represented, where, in particular, the filter systems and the spinneret at the end of the spinning process were studied in detail, using the possibilities of Computational Fluid Dynamics (CFD).[4] Modeling for falling film evaporators for a heat pump has been reported, based on the classical Newton's viscosity law and Nusselt's falling film theory.[5]

The flow pattern in an agitated thin film evaporator has been analyzed using ANSYS-CFX 10.0 software, where the bow wave in front of the tip of blade near the inner wall is simulated using the free surface multiphase model, considering two continuous phases: water and water vapor.[6]

The research focusing on VWFEs is very extensive all over the world,[7-15] however, to the best of the authors' knowledge, there are only a few published results on the simulation for the evaporation process of the Lyocell solution in the

VWFE.[4,16] Moreover, there seem to be no papers focusing on reed Lyocell solution.

In this paper, under some assumptions about the Lyocell solution, we establish a mathematical model considering the rotation of the axis for the process of evaporation dissolution of a Lyocell solution in the VWFE, and represent the numerical simulation analysis for the flow profile, pressure, residence time, interior temperature considering friction heat and mass concentration of the solution in VWFE. The Turbulent Flow model in geometries with rotating parts and the frozen rotor approach, as well as the level set module in COMSOL Multi-physics 5.4, were used for simulation of the flow pattern of the solution in the VWFE. Moreover, for the simulation of temperature distribution and mass fraction distribution of the solution in the VWFE, the heat transfer and mass transfer model were used. Comparing the obtained simulation results with experimental details, the reliability of our simulation method is shown.

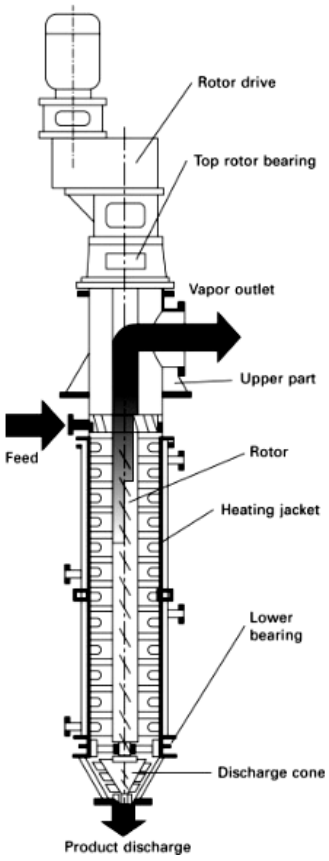

Figure 1: General structure of VWFE

Evaporation dissolution process of Lyocell solution in VWFE

In the Lyocell process, the operation of the VWFE is implemented as follows. The mixture formed through the swelling process, consisting of 75 percent NMMO solvent and cellulose, mixed so as to ensure that cellulose is scattered as uniformly in the solvent as possible, is supplied through the feed input continuously into the evaporator. The temperature of the interior wall of the VWFE is kept in the range of 80~85 °C by passing the heated vapor to 90 °C into the heating jacket.

Meanwhile, the interior of the VWFE is kept in a vacuum state (about 730 mmHg) by using a vacuum pump, so that the boiling point should be lowered by more than 20 °C, compared to the temperature of the solution. In this state, if the mixture of solvent, water and cellulose heated to 80~85 °C is introduced into the evaporator through the feed input, it is smeared on the surface of the interior wall with a thin thickness (about 2~5 mm) by the rotating agitator blade and, at the same time, the water in the mixture is evaporated explosively. Also, by the rotating agitator blade, the mixture is agitated and moved

downward continuously, and on the course of the mixture's moving downward, the water is still evaporated and cellulose is dissolved in the solvent. Completed products are discharged through the product outlet by the discharge cone blade and screw. Meanwhile, the volatile gas, including the evaporated steam, is exhausted to the evaporation gas outlet by the vacuum pump.

The criterion from the viewpoint of the operation of VWFE is to decrease the content of water in the mixture for spinning from the initial 20 percent to 10 percent.

Mathematical modeling for the evaporation dissolution process in VWFE

First of all, for the facilitation of the mathematical model for the evaporation dissolution process in the VWFE, some assumptions should be made:

- The motion of the mixture (solution, volatile gas) is treated as fluid flow in the interior of VWFE. In other words, the process through which the solution turns into the solid state is not considered;
- There is no interaction between the solution and the vapor;
- In the simulation for the mass fraction of the volatile gas, only the vapor is considered;
- The evaporation occurs only in the water in the mixture and in the whole domain filled with the mixture, not only on the surface, due to the agitation.

The motion of the mixture in the VWFE can be represented by the following fluid flow equations for rotating fluids:[17,18]

$$\mathrm{div}u = 0 \tag{1}$$

$$\rho\frac{\partial u}{\partial t} + \rho(u\cdot\nabla)u + 2\rho\psi\times u + \nabla p = \mu\Delta u + f - \rho\left(\frac{\partial\psi}{\partial t}\times r + \psi\times\psi\times r\right). \tag{2}$$

where $\rho[kg/m^3], \mu[Pa\cdot s]$ are the density and viscosity of the mixture, respectively, and u the linear velocity of the mixture in the VWFE, $p[Pa]$ – the interior pressure, $\psi[rpm]$ – the angular velocity vector, $r[m]$ – the distance to the considered point from the rotating axes. The density of the mixture can be defined as follows:

$$\rho = \rho_1\cdot v_1 + \rho_2\cdot v_2 + \rho_3\cdot v_3 \tag{3}$$

where $\rho_i[kg/m^3], v_i[1], i = 1,2,3$ are the density and volume fraction of cellulose, NMMO solvent and water, respectively. The density of vapor is too small, so that it is negligible in the computation of the flow of the mixture. Because there is no viscosity model for mixtures reported in the literature, we have defined it by using the continuous viscometer and have presented the experimental results in Table 1.

For the numerical solution of Equations (1) and (2), the frozen rotor approach in COMSOL Multi-physics 5.4 was used. We divide the whole domain into two parts: the non-rotating domain and the rotating domain (Fig. 2). In general, the rotating domain is set so that it should be included in the whole domain and envelop all agitator blades, cone blades and rotating axes. We couple individual equations on the rotating, non-rotating domains by the continuity conditions for u and p on the contact boundary:

$$u_{non\_rot} = u_{rot},\ p_{non\_rot} = p_{rot} \tag{4}$$

where $u_{non\_rot}, u_{rot}, p_{non\_rot}, p_{rot}$ are the velocity and pressure on the contact boundary in the non-rotating and rotating domains, respectively. On the wall of the VWFE, no slip condition is set,[5] and the feed inlet velocity is given on the feed inlet boundary. On the product outlet boundary, the output pressure of the solution is set and vapor flow velocity measured by experiment is given on the vapor outlet boundary.

The flow pattern between the solution and the blades in the VWFE is simulated using the level set model, considering two continuous phases: solution and vapor.

Table 1
Experimental values for viscosity on component and temperature of mixture

Cellulose concentration (wt%)	Temperature (°C)	Viscosity (Pa·s)
7	80~100	5000~3000
9	80~100	6000~5000
9.5	73~78	9000~6000

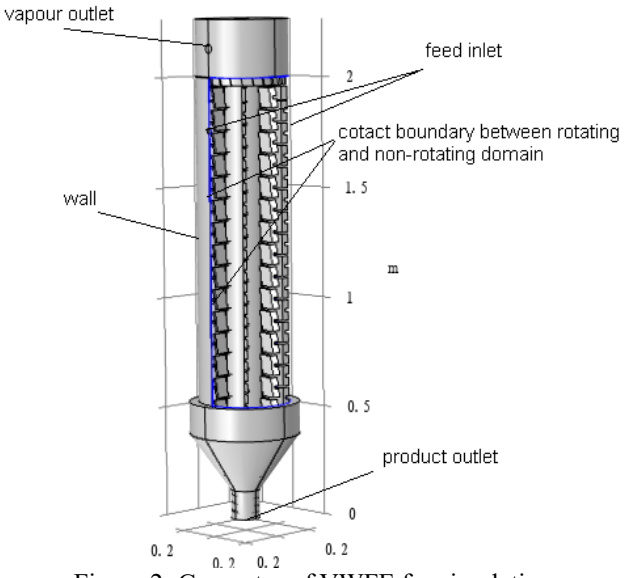

Figure 2: Geometry of VWFE for simulation

Table 2
Data used for simulation

Parameters	Value	Unit
Feed speed	20	kg/h
Rotor speed	120	rpm
Density of reed	1100	kg/m^3
Density of nmmo	1200	kg/m^3
Specific heat capacity	1.9	kJ/(kg·K)
Latent heat of evaporation	2432.21	kJ/kg
Cellulose concentration	7	wt%
Nmmo concentration	73	wt%
Water concentration	20	wt%
Feed, jacket temperature	80	°C
Vacuum factor	4000	Pa
Coefficient of heat conduction	0.11	W/(m·K)

Numerical analysis results in VWFE

We implemented numerical simulation for the Lyocell solution made from reed as raw material and compared the obtained results with experimental data. For the simulation, COMSOL Multi-physics 5.4(2018) was used. The data used for simulation are exhibited in Table 2.[1,19,20]

Flow of mixture in VWFE

We implemented the flow simulation of the solution considering a gap between the part of the cylinder and the blade of about 5 mm. The purpose in this simulation has been to show that when the vacuum state is kept by pulling out vapor flow to the top of the VWFE by the vacuum pump, the flow of the solution is not turned to the rotating axes. In Figure 3, the flow velocity and streamline of the solution and the pressure impressed on the blades are shown. From Figure 3, we can find out that the solution rotates and flows down with maximum linear velocity 2.57 m/s, and the agitator blades are given the pressure of 4000 Pa.

Next, we show the velocity distribution and streamline of the mixture in the section of the cylinder part (Fig. 4). In Figure 4, the volume fraction distribution of the solution is shown approximately in the section of VWFE. From the analysis of Figures 3, 4 and 5, we can find out that the solution is spread on the interior wall of the VWFE and flows down, and the flow of the solution is not turned to the rotating axes.

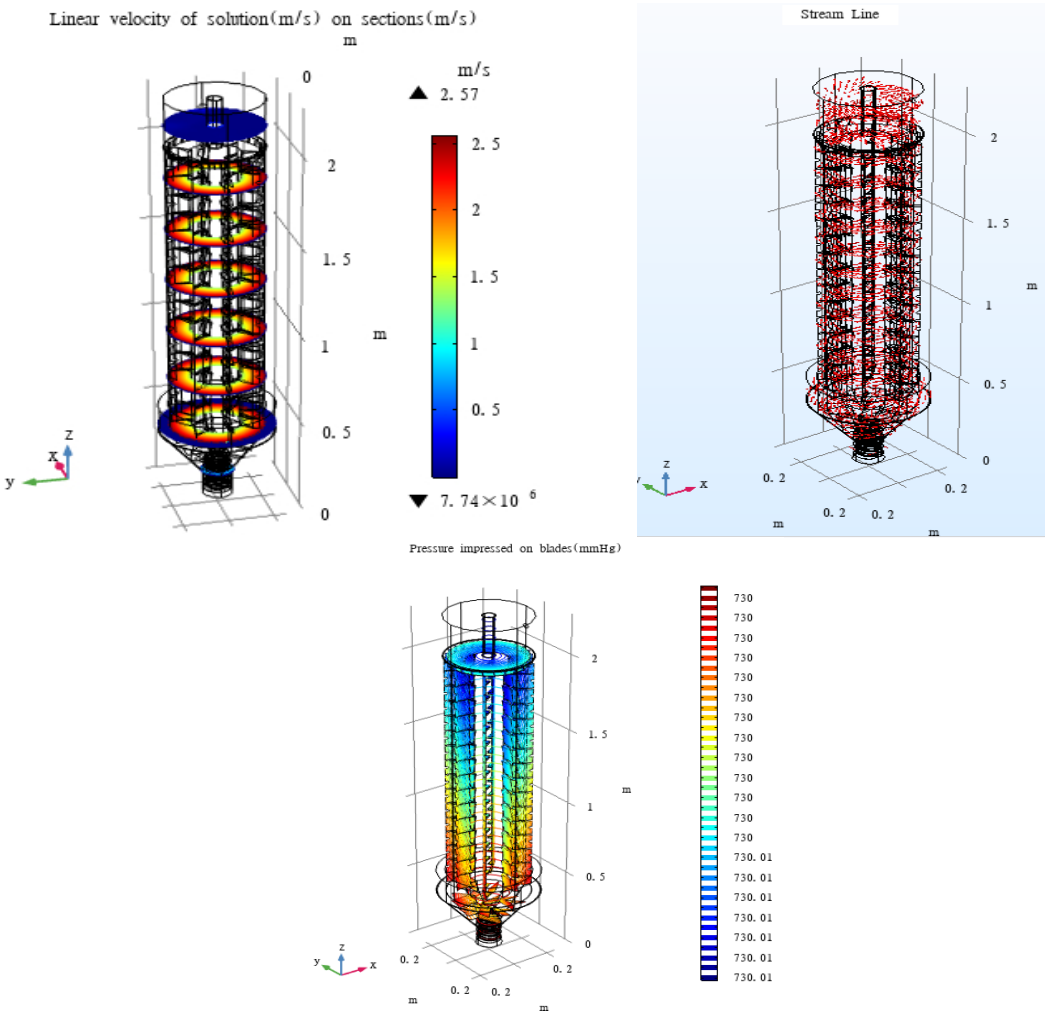

Figure 3: Flow velocity, streamline of solution and pressure impressed on blades

Residence time of solution in VWFE

The residence time of the solution in the VWFE can be computed by the downward flow velocity on the contact boundary between the rotating and the non-rotating domain (Fig. 6). From these results, we can find that the mean downward flow velocity is about 0.08 cm/s and, therefore, the residence time is about 42 min. After the implementation of several simulations according to different rotor speed levels (40 rpm, 80 rpm, 120 rpm), we can conclude that the residence time of the solution in the VWFE is mainly dependent on the feed speed of the mixture, not on the rotor speed. These facts are in agreement with the experimental results.

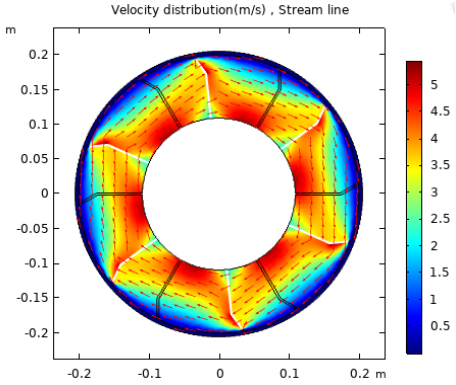

Figure 4: Velocity distribution and streamline of mixture in the section of cylinder part

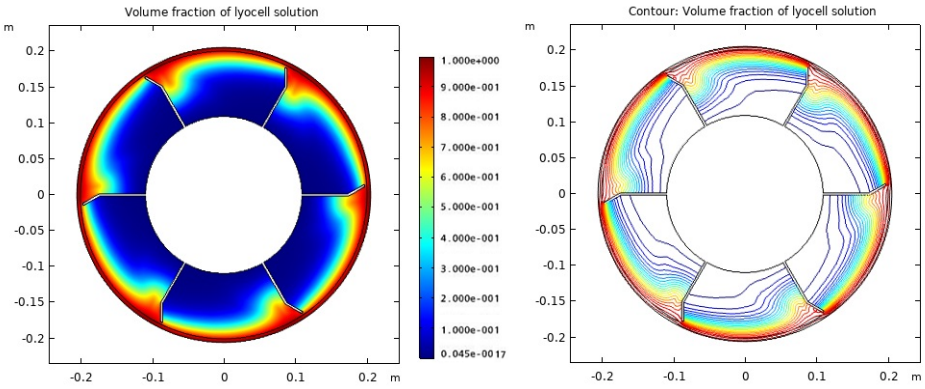

Figure 5: Volume fraction distribution of solution

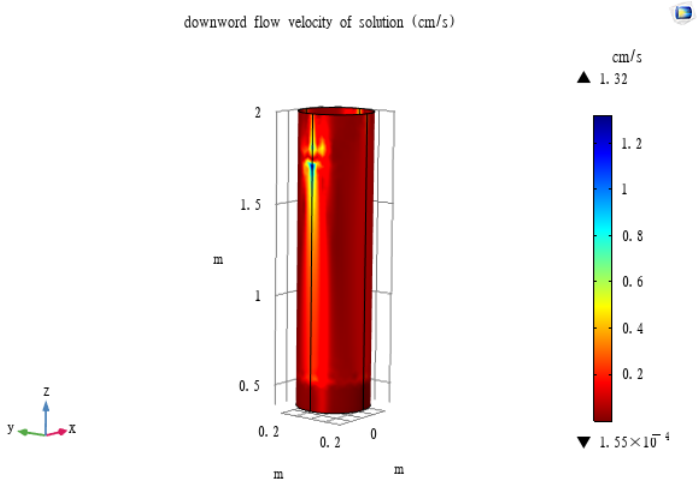

Figure 6: Downward flow velocity distribution of solution on the contact boundary between the rotating and non-rotating domain

Validation of simulation

Closely coupled with an accurate formulation of the problem is the validation of the model and of the accuracy of the computations.

Mesh convergence

Because a direct comparison of numerical values of the simulation with the analytic solutions of the model is impossible, the convergence of numerical results was verified through mesh convergence, going up to 53102 mesh vertices, 268988 elements, to achieve a numerically accurate and converged solution. The effects of changing the number of vertices and elements, as shown in Table 3, for the linear velocity and the downward flow velocity distribution, give an absolute error of 10^{-5}. Tests were carried out with finer meshes, but no influence on the results was observed. The input parameters used in this study are shown in Table 2.

Table 3
Number of vertices and elements used to test mesh convergence

Number of vertices	Number of elements
11291	107926
25854	125100
30059	143938
53102	268988

Table 4
Comparison of residence time

Feed speed, kg/h		20			36		
Rotor speed, rpm		40	80	120	40	80	120
Residence time, min	Simulation	42	44	41	27	27	28
	Experiment	42	42	42	27	27	27

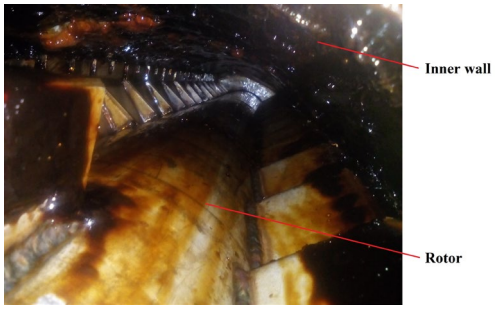

Figure 7: A photo of the inner wall condition of the experimental apparatus after experiments

Comparison with experimental results

In order to test the reliability of our simulation, we compared simulation results with the experimental results obtained for the VWFE.

The structure of the experimental apparatus that we made and used is the same as shown in Figure 1. The inner cylinder is 1747 millimeters high, 407 millimeters in diameter, and the height from the bottom of the cylinder to the feed input is 1489 millimeters. The heating jacket was divided into four steps and the discharge cone was also covered with the heating jacket. In this set-up, five jackets and a temperature sensor (WZP-231) were installed, respectively. In order to measure the temperature and pressure (degree of vacuum) in the apparatus, a temperature transducer (SBWZ-TH02EX/44sKi) and an absolute pressure transducer (EJA310A-DMS5A -22EA) were installed on the lid. The rotating speed of the rotor was controlled by using an inverter (FR-F72011K) and the actual numbers of rotation were measured by an incremental encoder (XH3806-1024/5-24C).

We implemented some experiments by changing the feed speed and the rotor speed in this experimental apparatus. We used 20 kg/h and 36 kg/h for the feed speed, and 40 rpm, 80 rpm and 120 rpm for rotor speed, respectively. We kept the interior pressure to 4000 Pa and the temperature of the jacket to 80 °C. For these operation parameters, we measured the residence time and compared it with the values from the simulation for the feed speed of 20 kg/h and 36 kg/h, respectively. Table 4 exhibits the results.

Also, in order to confirm that the solution was plastered on the inner cylinder wall, we dismantled the apparatus after the experiments and observed its inner condition. Figure 7 presents a photo of the inner wall. As may be noted in the photo, the Lyocell solution is spread on the inner wall and the flow of the solution is not toward the rotating axes during the evaporation and dissolution process. Through these comparisons and observations, we can conclude that our simulation corroborates the flow process of the Lyocell solution in VWFE beautifully.

CONCLUSION

A mathematical simulation was performed for the vacuum evaporation dissolution process of a Lyocell solution (reed cellulose, NMMO solvent, water) in the VWFE. From our simulation, some conclusions for the flow process of the Lyocell solution in the VWFE were obtained.

First, during the evaporation and dissolution process, the solution is spread on the interior wall of the VWFE and flows down, and the flow of the solution is not toward the rotating axes. Also, the residence time of the solution in the VWFE is mainly dependent on the feed speed, and not on the rotor speed.

In future work, we plan to describe simulation results for temperature distribution and mass fraction distribution of the Lyocell solution in the VWFE.

REFERENCES

[1] H. Sixta, Postgraduate course on Cellulose Chemistry Lyocell Fibers, Aalto University School of Chemical Technology, 2016, pp. 21-22

[2] R. H. M. Azzam, *Elixir Int. J.*, **151**, 55229 (2021),

https://www.elixirpublishers.com
[3] A. A. Al-Hemiri, E. F. Mansour and J. A. L. Al-Ani, *Iraqi J. Chem. Petrol. Eng.*, **9**, 43 (2008), https://doi.org/10.31699/IJCPE.2008.2.5
[4] M. H. Bouwman, "Multiphase Simulations of a Lyocell Process", LAP Lambert Academic Publishing, 2008, https://digitalcollection.zhaw.ch/handle/11475/6079
[5] A. de la Calle, L. J. Yebra and S. Dormido, in *Proceedings of the 9th International Modelica Conference*, September 3-5, 2012, Munich, Germany, p. 3, https://doi.org/10.3384/ecp12076941
[6] B. Pawar Sanjay, A. S. Mujumdarb and B. N. Thorat, *Chem. Eng. Res. Design*, **90**, 757 (2012), https://doi.org/10.1016/j.cherd.2011.09.017
[7] J. Cvengroš, Š. Pollák, M. V. Micov and J. Lutišan, *Chem. Eng. J.*, **81**, 9 (2001), https://doi.org/10.1016/S1385-8947(00)00195-9
[8] L. T. Jacinto, Ph.D. Thesis, The University of Texas, Austin, 2006
[9] S. J. Kulkarni *Int. J. Res. Rev.*, **2**, 10 (2015), https://www.gkpublication.in
[10] P. Saksena Nirav, *Int. J. Sci. Res. Develop.*, **4**, 1 (2016), https://www.ijsrd.com
[11] P. White, M. Hayhurst, J. Taylor, and A. Slater, in "Biodegradable and Sustainable Fibres", edited by R. S. Blackburn, Woodhead Publishing Series in Textiles, Woodhead Publishing, 2005, pp. 157-190, https://doi.org/10.1533/9781845690991.157
[12] S. Zeboudj, N. Belhaneche-Bensemra, R. Belabbes and P. Bourseau, *Chem. Eng. Sci.*, **61**, 1293 (2006), https://doi.org/10.1016/j.ces.2005.08.010
[13] T. Cebeci, "Analysis of Turbulent Flows", 2nd ed., Elsevier, Amsterdam, 2004, https://www.elsevier.com
[14] H. R. Kemme and S. I. Kreps, *J. Chem. Eng. Data*, **14**, 98 (1969)
[15] M. Luszczyk and S. K. Malanowski, *J. Chem. Eng.*, **51**, 1735 (2006)
[16] F. Rossi, M. Corbetta, D. Geraci, C. Pirola and F. Manenti, *Chem. Eng. Trans.*, **43**, 1429 (2015), https://doi.org/10.3303/CET1543239
[17] COMSOL Documentation, 2018, Theory for the Rotating Machinery Interfaces, https://www.comsol.com
[18] COMSOL Documentation, 2018, Theory for the Transport of Concentrated Species Interface, https://www.comsol.com
[19] M. Murru, G. Giorgio, S. Montomoli, F. Ricard, F. Stepanek, *Chem. Eng. Sci.*, **66**, 5045 (2011), https://doi.org/10.1016/j.ces.2011.06.059
[20] I. M. Smallwood, "Handbook of Organic Solvent Properties", Elsevier, 1996